ANNALI DI GEOFISICA, VOL. XXXVI, N. 1, April 1993

Aftershock location and *P*-velocity structure in the epicentral region of the 1980 Irpinia earthquake

Alessandro Amato and Giulio Selvaggi
Istituto Nazionale di Geofisica, Roma, Italia

Abstract
We relocated more than 600 aftershocks of the M_S 6.9 November 23, 1980, Irpinia earthquake recorded by a local network from November 26, 1980 to February 1981. We compared different one-dimensional velocity models and then computed a three-dimensional model using a damped least-square inversion procedure, starting from our best 1-D. The results of the inversion show that the Irpinia earthquake ruptured a strongly heterogeneous medium, which probably determined the complexity of the mainshock. Near the surface, the velocity anomalies agree with exposed geologic structures, mainly limestone units (high velocities) and terrigenous basins (low velocities). The velocity anomalies reflect the presence of lithological and/or rheological heterogeneities which may have strongly controlled the rupture propagation during the mainshock. The main rupture was probably driven by a sharp, NW-SE elongated velocity contrast, which is continuous at depth (approximately below ~6 km), but exhibits lateral variations near the surface. A good correspondence between shallow low velocities and gaps in surface faulting is found. The mainshock nucleated in a high-velocity region along a 60° dipping fault that probably steepens at about 7 km depth near the boundary between the stiff Apulian platform and the overlying Meso-Cainozoic sedimentary units. The volume of rocks directly overlying the mainshock shows a rarefaction of aftershocks, compared to the surrounding regions, possibly as an effect of the large moment released near the nucleation zone during the mainshock. The main northeast steeply dipping fault is associated with a secondary antithetic fault which ruptured 40 s after the nucleation. The velocity anomalies suggest that this southwest-dipping secondary normal fault reactivated a thrust of the pre-Pliocene Apenninic compressional regime.

1. Introduction

The velocity structure and the seismicity can be better analysed together in order to understand the active tectonic processes in a seismically active region. A three-dimensional velocity model of the crust can be obtained, using travel time residuals of local earthquakes. Such a model gives original information on the structure of the volume of the crust that produces the seismicity. In the upper crust, the velocity anomalies are mainly related to structural inhomogeneities. In seismogenic regions such inhomogeneities play an important role in the process of rupture propagation, which is controlled by the structural orientation and by the type of materials.

One of the main controversies regarding the 1980 Irpinia earthquake is the apparent discrepancy between its faulting mechanism and the regional geologic setting. In one side, geologists and geophysicists looked at surface and subsurface geology and reflection seismic profiles and pointed out that the structural setting of this region is dominated by northeast verging, southwest dipping, outcropping and blind thrusts (Mostardini and Merlini, 1986). The main normal faults recognized in this structural context from reflection lines are southwest-dipping listric faults, which flatten at depth joining ancient thrust planes (Casero *et al.*, 1988; Roure *et al.*, 1990). On the other hand, seismologists demonstrated that the 1980 Irpinia event, as well as many other instrumentally recorded earthquakes of the Central and Southern Apennines, had an almost pure normal faulting mechanism (Westaway and Jackson, 1987; Bernard and Zollo,

1989; Pantosti and Valensise, 1990; Giardini, this volume). Moreover, there is clear evidence from surface, geodetic and strong-motion data that the fault which ruptured during the mainshock was a northeast-dipping normal fault, likely together with an antithetic, blind, smaller southwest-dipping normal fault, which ruptured 40 s later (see fig. 1). Paleoseismological studies (Pantosti *et al.*, 1989) demonstrated that the 1980 fault has been active for several thousand years, in at least four seismic cycles. Nevertheless, the 1980 Irpinia fault had never been reported on neotectonic maps (Ambrosetti *et al.*, 1983). The contrast between geologic and seismologic observations is therefore surprising. The explanation of this apparent controversy is probably to be sought in the diachronism of the tectonic regimes. The extensional regime in Southern Apennines was probably established only after the thrusting system started to be uplifted. The crustal structures described by both surface and subsurface geology and from seismic profiles are the result of a compressional tectonic regime which has been active for millions of years, while seismological and even paleoseismological investigations look at fault structures which are active now, and in the case of this portion of the Apennines, only for some thousand years. A long time (and several seismic cycles) is needed before a normal fault becomes «visible» with classical geophysical studies.

2. Aftershocks of the 1980 event

A temporary microseismic network was installed a few days after the M_S 6.9 mainshock, allowing the recording of thousands of earthquakes. The aftershock distribution, together with the analysis of other data, provided additional constraints on the faulting mechanism (Deschamps and King, 1984; Westaway and Jackson, 1987; Bernard and Zollo, 1989).

In fig. 1 about 200 aftershocks recorded in the period 1-15 December 1980 are plotted in a map and on a cross-section (AA′) perpendicular to the fault. The CMT focal mechanism of the mainshock, the epicenters of its three main subevents, the location of the fault fragments inferred from surface and geodetic data and some interpretative features are also reported in fig. 1 (from Amato *et al.*, 1989 and Valensise *et al.*, 1989). Most of the aftershocks occurred between the two antithetic faults (fig. 1b)). As pointed out by Westaway and Jackson (1987), the determination of the shape of the main fault, which apparently steepens towards the surface, unfortunately suffers the inaccuracies in the mainshock location and in the true dip of the fault plane.

The identification of an almost continuous, ~40 km long fault scarp, first partly noticed by Westaway and Jackson (1987), then extensively mapped and studied by Pantosti and Valensise (1990), posed the problem of the relationships between fault rupture and crustal structure at depth. In other words: did the rupture originate in the Apulian basement and transmitted up to the surface? Are the slip variations observed at the surface related to the shallow crustal structure or to true inhomogeneities in the coseismic slip distribution, or to both? Was the main rupture propagation driven or controlled by the local crustal structure?

In order to get an insight on these aspects, we computed a 3-D velocity model using Thurber's (1983) inversion technique of local earthquake travel time residuals, as extended by Eberhart-Phillips (1989). We used different datasets consisting of a different number of selected aftershocks (~65, ~200, ~650) to evaluate the stability of the results.

As briefly discussed here, it is important to start a 3-D inversion with a good initial homogeneous model. To do this, we started with a good half-space velocity model; then we compared the half-space and some 1-D layered models published by different authors (Deschamps and King, 1984; Bernard and Zollo, 1989) (table I). We first selected the best-fit half-space among several models, following the procedure used by Aster (1986), observing the weighted-mean residual for P and S phases and the associated weighted standard deviations. The best half-space velocity model for the Irpinia region was calculated using 100 selected aftershocks with at least 8 P readings with full weight and 5 S readings, using Hypoinverse (Klein, 1989). The best-fit half-space obtained with this procedure (table I) represents the model that best averages the velocity characteristic of the crustal volume beneath the

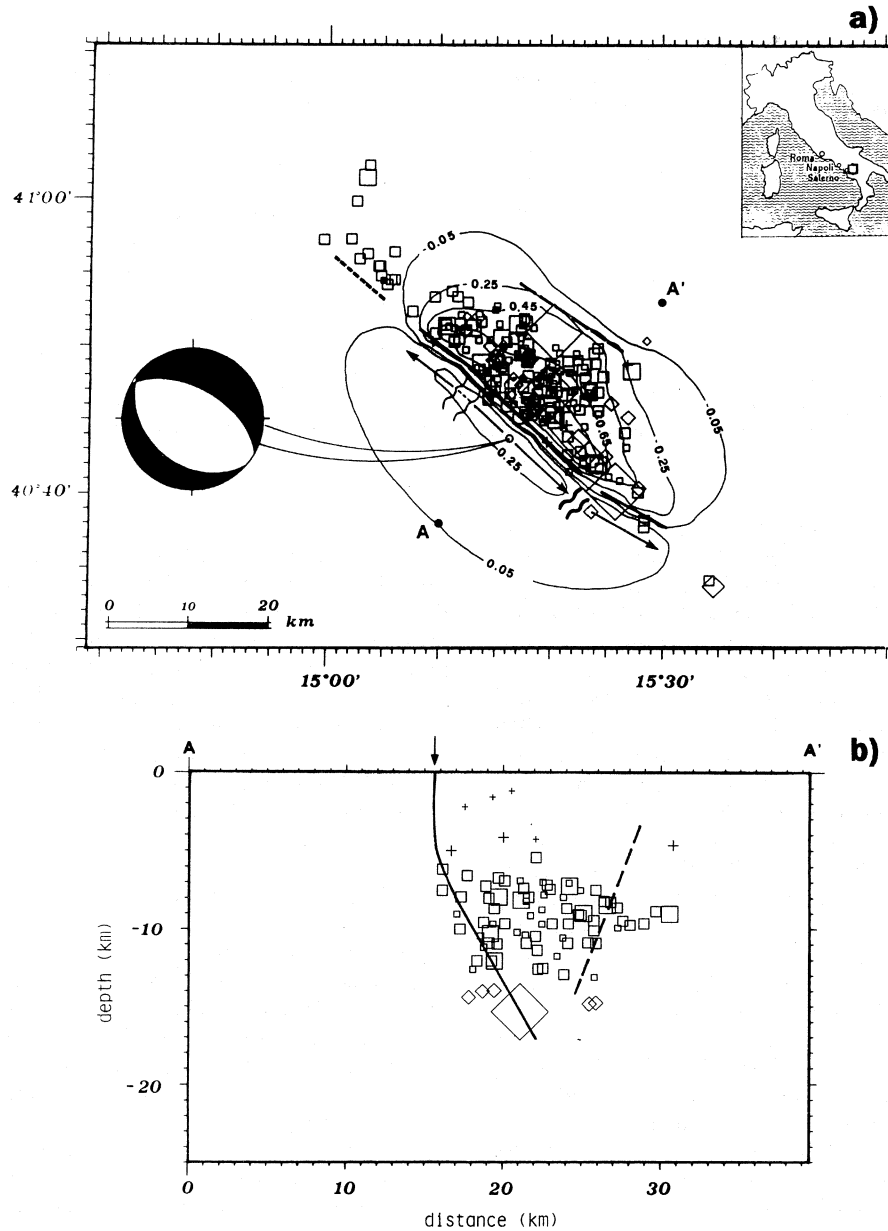

Fig. 1. a) Interpretative model of the Irpinia earthquake (from Amato *et al.*, 1989). About 200 aftershocks are plotted, together with the focal mechanism of the mainshock, the three main subevents (the larger squares), the four proposed fault fragments, mainly constrained by surface and leveling data (Pantosti and Valensise, 1990) and strong-motion recordings (Bernard and Zollo, 1989). The arrows indicate the direction of the rupture propagation, interrupted by two barriers (≈) (a strong barrier to the southeast, and a «relaxation» barrier to the northwest). The isolines are the elevation changes predicted by the model. b) The arrow indicates the fault scarp and the dashed line represents the hypothesized antithetic fault.

Table I. 1-D velocity model for the studied area.

Half-space model		Deschamps and King model		Bernard and Zollo model		Amato and Selvaggi model	
V_P (km/s)	h (km)	V_P (km/s)	h (km)	V_P (km/s)	h (km)	V_P (km/s)	h (km)
5.10	0.0	4.50	0.0	2.27	0.0	4.50-2.65*	0.0
		5.50	3.0	5.32	3.0	4.50	3.0
		6.50	13.0	6.03	7.0	5.70	6.0
				6.28	10.0	6.50	10.0
				6.54	20.0	7.50	25.0
$V_P/V_S = 1.78$		$V_P/V_S = 1.81$		$V_P/V_S = 1.78$		$V_P/V_S = 1.81$	

* The two V_P values are relative to the southwestern (4.50 km/s) and the northeastern (2.65 km/s) regions.

network. It cannot provide any information on the geological structures, but only on the degree of heterogenity of this volume of rock.

Figures 2a) and 3a) show the aftershock locations of the events with horizontal errors less than 1.0 km and vertical errors less than 2.0 km, selected from about 1000 earthquakes recorded by at least 8 stations from November 26, 1980 to February 1981. These locations were obtained using the selected half-space velocity model.

We compared the aftershock locations obtained with the current 1-D velocity models (Deschamps and King, 1984; Bernard and Zollo, 1989), always using the same dataset (table I, fig. 2b), c) and 3b), c)). Then, we obtained a new 1-D model (table I) considering the two quoted models and the information inferred from the seismic reflection section of Mostardini and Merlini (1986). In addition, as the stations to the northeast showed systematic positive delays up to almost 1 s, we introduced a low-velocity layer for the upper 3 km for the northeastern region, as also suggested by geological evidence (Mostardini and Merlini, 1986).

Figures 2 and 3 show the locations of the events with horizontal error less than 1.0 km and vertical error less than 2.0 km located with the four models shown in table I. There are only slight differences in the locations. The main differences are found on the depth parameter, that is affected by the position of the different discontinuities of the 1-D models (fig. 3a)-d) and table I).

The events located with the low-velocity layer at the surface (fig. 2d) and 3d)) show a systematic shift to the northeast, allowing a better delineation of the map trace of the fault (fig. 2d)), although no clear evidence of the 60° fault dip appears from the cross-section (fig. 3d)), as already pointed out by Virieux *et al.* (1988). It is interesting to observe that the aftershocks are spread in the whole volume between the main and the antithetic fault proposed by Bernard and Zollo (1989) (fig. 2 and fig. 3), without clearly delineating any fault plane.

3. 3-D inversion method

The inversion technique used to compute the three-dimensional velocity structure is that originally developed by Thurber (1983) and improved by Eberhart-Phillips (SIMULPS, unpublished Fortran program; 1989). It is based on a damped least-square inversion procedure and parameter separation (Pavlis and Booker, 1980) between hypocenter and velocity parameters.

The method is based on the linearization of the line integral for each arrival time, calculated along the source-receiver ray path. According to the ray theory, each arrival time can be described as

$$t = t_0 + \int_{\text{source}}^{\text{station}} \frac{1}{V(x,y,z)}\, ds$$

where t_0 is the origin time, $V(x,y,z)$ is the velocity

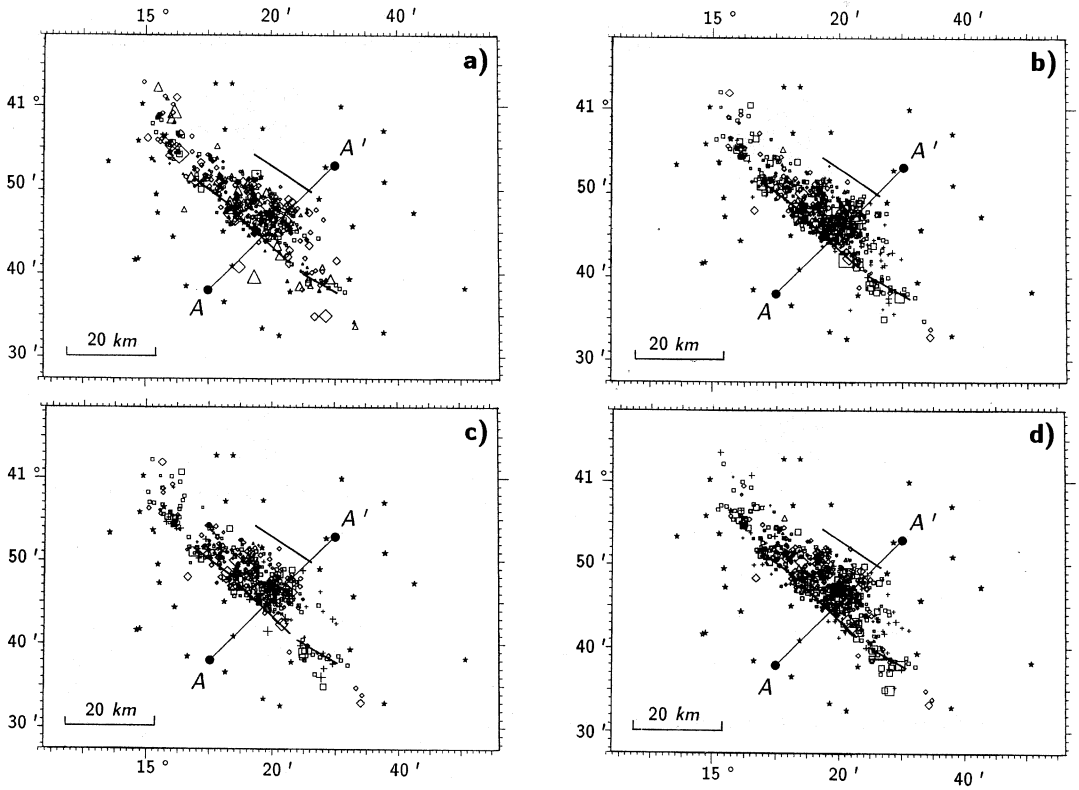

Fig. 2. Epicentral distributions for the velocity models of table I. a) Best-fit half-space; b) 1-D model derived by Deschamps and King (1984); c) 1-D model from Bernard and Zollo (1989); d) our 1-D model. The stars locate the seismic stations, the thin lines are the four fault segments proposed by Bernard and Zollo (1989) and Pantosti and Valensise (1990). AA′ is the trace of the vertical sections of fig. 3. See fig. 7 for earthquake symbol size and type.

function, and the line integral is calculated along the ray path.

Then, the linearized equations relating each arrival time residual Δt to the earthquake parameter variations Δx_E, Δy_E, Δz_E and to the velocity changes Δv_j can be written as

$$\Delta t = \frac{\partial t}{\partial t_0}\Delta t_0 + \frac{\partial t}{\partial x_E}\Delta x_E + \frac{\partial t}{\partial y_E}\Delta y_E + \frac{\partial t}{\partial z_E}\Delta z_E + \sum_{j=1}^{N}\frac{\partial t}{\partial v_j}\Delta v_j$$

The model is parameterized using a three-dimensional grid where each node is an assigned velocity value. The velocity in a generic point of the model is calculated by linear interpolation between adjacent nodes. In order to calculate the theoretical travel times, SIMULPS makes use of the ray tracer ART2 (Thurber, 1983), which allows accurate travel time estimates when source-receiver distances are within a few tens of kilometers. Using this algorithm, ray paths between sources and receivers have fixed circular arc shapes, and are then perturbed by a «pseudo-bending» procedure (Thurber, 1983, Eberhart-Phillips, 1989).

The whole inversion procedure can be summarized as follows:

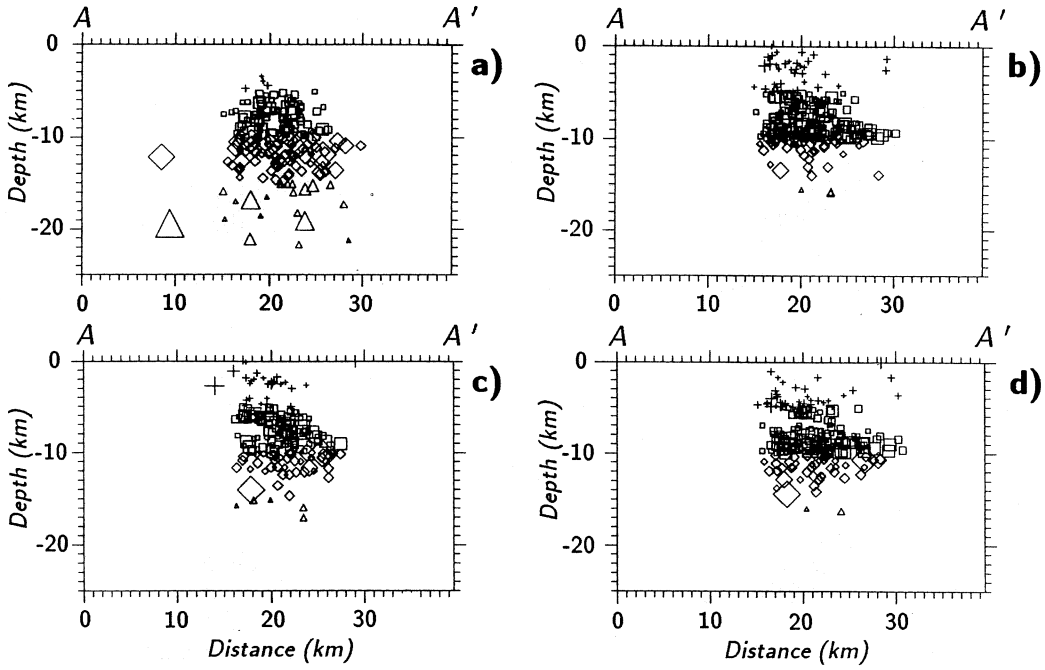

Fig. 3. Cross-sections of the epicentral distributions of fig. 2.

a) Definition of a homogeneous starting model. In our case, we used the last model of table I.

b) Hypocenter location using the homogeneous starting model. We present here the results relative to a set of about 600 earthquakes.

c) Computation of the velocity perturbations to the initial model (damped least-square inversion). The choice of the damping parameter is made by performing preliminary one-iteration runs with different damping parameters; the best damping value is that resulting in the greatest data-variance reduction without increasing the solution length too much. Figure 4 shows the trade-off curve obtained applying this procedure to the Irpinia dataset for the 3-D model shown in the next section. The selected value is 200 $s^2/(km/s)^2$.

d) Earthquake relocations with the updated 3-D model. Points a) through d) are iteratively repeated until the data variance reduces significatively, according to an F-test.

4. The 3-D inversion results

In the computation of the velocity model, we tried to achieve a greater detail with respect to our previous attempts (Amato *et al.*, 1989; Amato and Selvaggi, 1990), using a greater number of earthquake travel times. We used 612 aftershocks recorded by at least 8 stations (~9000 *P* arrival times), and calculated the *P* velocity at 0, 3, 6, 9 km depth, with a horizontal gridspacing of 5 km in the middle of the investigating region. The gridspacing was optimized looking at the off-diagonal elements of the resolution matrix in each node for models with different grid spacing (Amato *et al.*, in preparation). For gridspacing smaller than 5 km there is a contamination between adjacent nodes, particularly along the preferred directions of ray propagation (*i.e.* the upper (2÷3) km below the stations, etc.).

We show here only the results at 3, 6 and 9 km depth. The poor ray density below the predominant hypocentral depth (~(5÷12) km, fig. 3d))

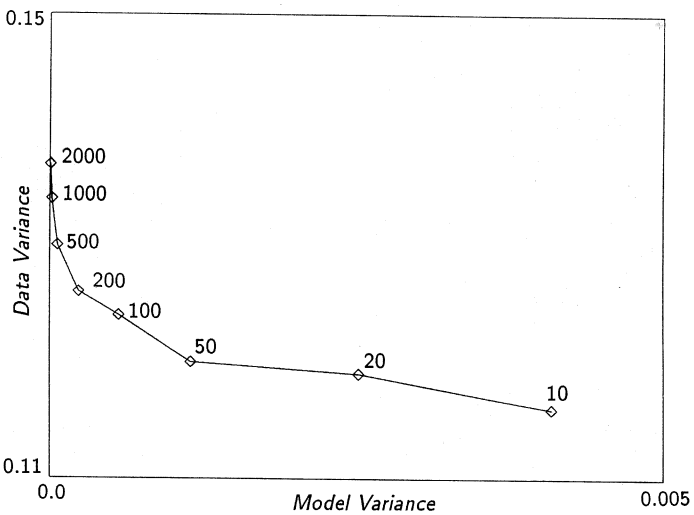

Fig. 4. Trade-off curve for the selection of the damping parameter for the 3-D inversion. Each point on the curve represents one inversion done with the indicated value of damping. We adopted a value of 200, a conservative choice that should ensure the linearity of the inversion.

prevents the computation of the velocity anomalies at greater depth.

As already pointed out by Amato and Selvaggi (1990), the velocities in the upper layers are strongly influenced by the surface geology. In particular, the sedimentary basins of the Ofanto River (to the East) and Sele Valley (fig. 5a)) approximately correspond to low velocities in the first layer, as expected.

The high-velocity anomalies at 3 km depth (fig. 5b)) are probably due to the presence of the limestone units of the buried Campania platform (Mostardini and Merlini, 1986). The low-velocity anomalies are determined by the basin of the Ofanto River, to the east, and by the north-south trending Sele Valley, that separates two high-velocity regions (fig. 5b)). As already pointed out by Bernard and Zollo (1989) and by Cocco and Pacor (this volume) based on strong-motion data, the region of the Sele Valley delayed the northwestward propagation of the rupture by ~2 s. Furthermore, Pantosti and Valensise (1990) found no surface slip in this region, which was interpreted as due to the presence of a «relaxation barrier». The existence of low velocities up to ~(5÷6) km depth suggests that the supposed Sele barrier is determined by a lateral heterogeneity.

At greater depth, the prominent feature in the velocity distribution is the abrupt contrast between the high velocities in the southwestern region and the low velocities in the northeastern sector (fig. 5c) and 5d)).

The location and strike (~NW-SE) of the boundary between high- and low-velocity regions (fig. 5b)-5d)) approximately correspond to the position at depth of the normal fault which ruptured during the mainshock (*strike* ~314°, *dip* ~60°, see fig. 1). According to Westaway and Jackson (1987) the mainshock is located at ~10 km depth, right below the depth where we detected the described abrupt velocity change (fig. 5c) and 5d)). The main rupture propagated close to the boundary between the high- and the low-velocity zone, probably within the former. This suggests the existence of a discontinuity at depth that might have driven the rupture process.

The high-velocity region observed at 9 km depth (fig. 5d)) seems to coincide with the extent of the main rupture (the so-called *0 seconds* rupture, Bernard and Zollo, 1989), that includes the two sub-segments of M. Marzano and M. Cervialto, for a total length of about (25÷30) km. This might indicate that the main rupture involved a patch characterized by a velocity higher

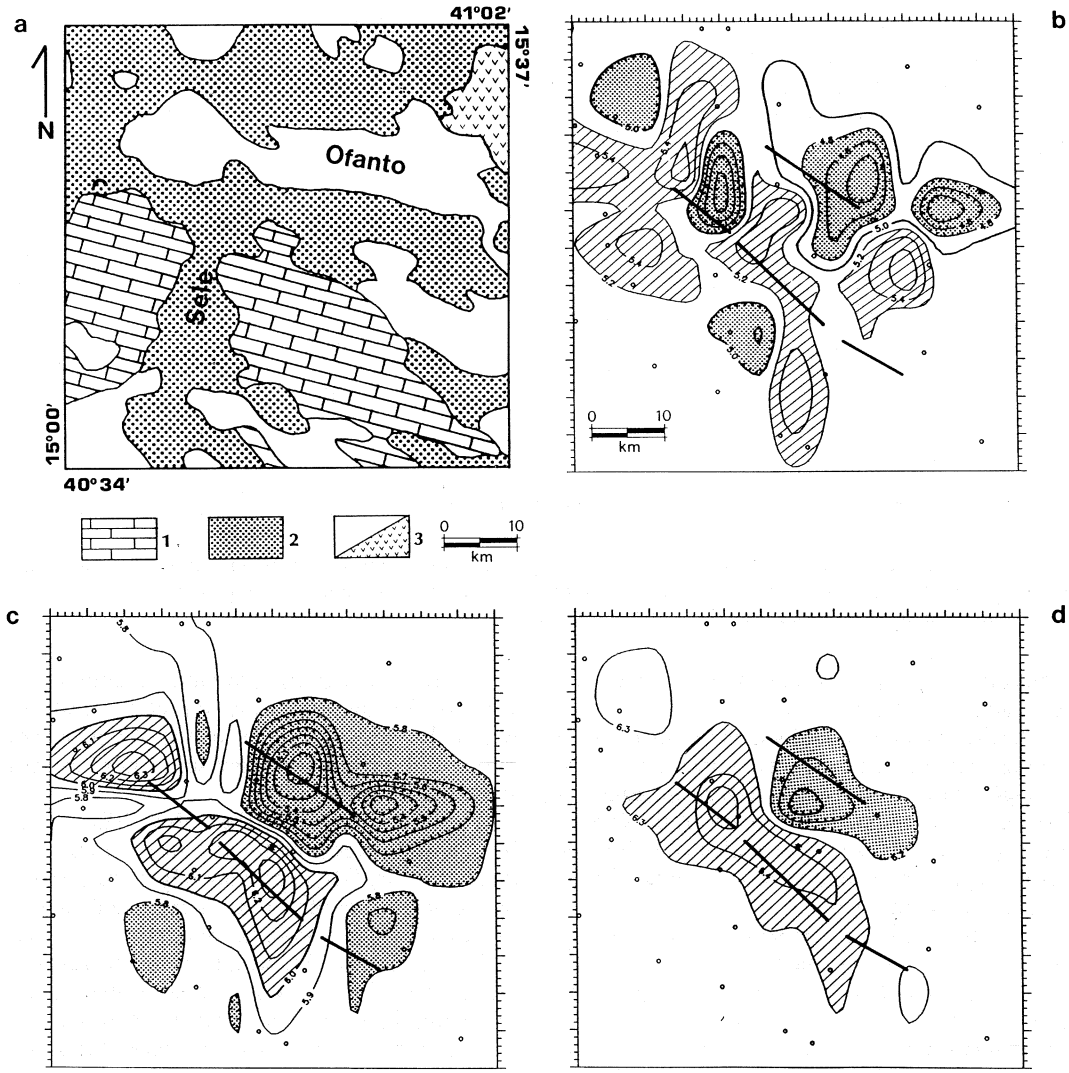

Fig. 5. a) Simplified geologic map of the Irpinia region. 1) Meso-Cainozoic limestones of the Campania platform; 2) terrigenous and flyschoid formations; 3) Plio-Pleistocene sediments (V's indicate the volcanic rocks of the Vulture Mtn.); b), c) and d) are the *P*-velocity anomalies at 3, 6, and 9 km depth, respectively; the dashed areas represent high velocities, the dotted zones represent low velocities.

(and hence stiffer) than the surrounding regions. The relocated aftershocks show that seismicity is spread in volume rather than being concentrated on a linear discontinuity (fig. 6a) and 7), which confirms the complexity of this event. It is interesting to observe that the strongest aftershocks are located close to the edges of the adjacent sub-segments that ruptured during the mainshock (fig. 6b)), suggesting that the existence of such sub-segments is determined by pre-existing lithological discontinuities, where the stress concentrated after the mainshock.

The aftershocks relocated with the 3-D model tend to move towards the low-velocity region, although the locations are not very different from those obtained with a 1-D model and station delays.

5. Discussion

The velocity distribution at depth, in combination with the relocated aftershocks, provides new constraints in the interpretation of this complex earthquake.

One of the most controversial points is the misagreement between the 60° dip of the main fault (see Giardini, this volume), and the position of the surface rupture (Pantosti and Valensise, 1990). In fact, a planar fault connecting the hypocenter of Westaway and Jackson (1987) with the surface would appear some kilometers southwest of the actual position of the fault scarp. In order to explain this, Westaway and Jackson proposed different mechanisms of bending for the plane from about 10 km, the nucleation depth, up to the surface. Any interpretation is however affected by the uncertainties related to the poor location of the mainshock, which is estimated to be of about 3 km.

Looking at a cross-section perpendicular to the main fault (fig. 8a)), a zone with only a few aftershocks is visible between the mainshock and the surface trace of the fault. This rarefaction of the seismicity delineates the zone of largest moment release during the mainshock. In our interpretation, the rupture started at about 10 km depth, over a 60° dipping plane, as suggested by Westaway and Jackson (1987), which steepened to become almost vertical in the upper (6÷7) km (fig. 8a)). The nucleation occurred in a high-velocity region, probably within the stiff Apulian platform, and the rupture might have bent entering the less rigid Meso-Cainozoic sedimentary sequence. Most of the aftershocks occurred in the hanging wall of the main fault, between this and the antithetic normal fault thought to be responsible for the 40-s shock (Bernard and Zollo, 1989). On the basis of the velocity distribution along the transversal section (fig. 8a)), we interpret this latter fault as a reactivated northeast-verging thrust, inherited by the pre-Pliocene compressional tectonics of the Southern Apennines.

Comparing the seismicity and the velocity distribution along the main fault with the amount of surface slip measured by Pantosti and Valensise (1990) (fig. 8b)), we observe that the seismicity is concentrated beneath the Marzano-Valva sub-segment, where the largest slip (~1 m) was measured. From the inversion of strong-motion data, Cocco and Pacor (1992) found that the maximum slip at depth occurred in the same region. The Marzano sub-segment is bounded by two other clusters of seismicity, one deepening beneath the Sele Valley, to the northwest, and the other, almost vertical, in correspondence with the sudden drop of surface slip towards the Carpineta sub-segment (fig. 8b)). These two regions probably represent lithological discontinuities, where stress concentrated after the main rupture. This is also confirmed by the distribution of the strongest aftershocks, that are mostly clustered near the boundaries between the different sub-segments of the main fault, as shown in fig. 6b).

The Sele Valley (fig. 8b)) was interpreted either as a strong barrier by Bernard and Zollo (1989), based on strong-motion recordings, or as a relaxation barrier by Pantosti and Valensise (1990). Both Bernard and Zollo and Cocco and Pacor (1992, and this volume), found a time delay and a jump in the rupture velocity northwestward propagation of the rupture in correspondence of the Sele Valley, where no surface slip was observed (fig. 8b)). Approximately in the same region we found a strong low-velocity anomaly in the upper ~7 km, coincident with a lack of seismicity (fig. 8b)). Combining these two observations, we suggest that the upper ~7 km of the crust beneath the Sele Valley represent a creeping section of the Irpinia main fault, probably associated with a lithological (and rheological) discontinuity.

6. Concluding remarks

The three-dimensional velocity model shows that the 1980 Irpinia earthquake occurred in a strongly heterogeneous medium, which determined the complexity of the mainshock. The velocity anomalies are mainly due to lithological heterogeneities, at least in the upper (6÷8) km, that probably controlled the rupture propagation during the mainshock. The main rupture was

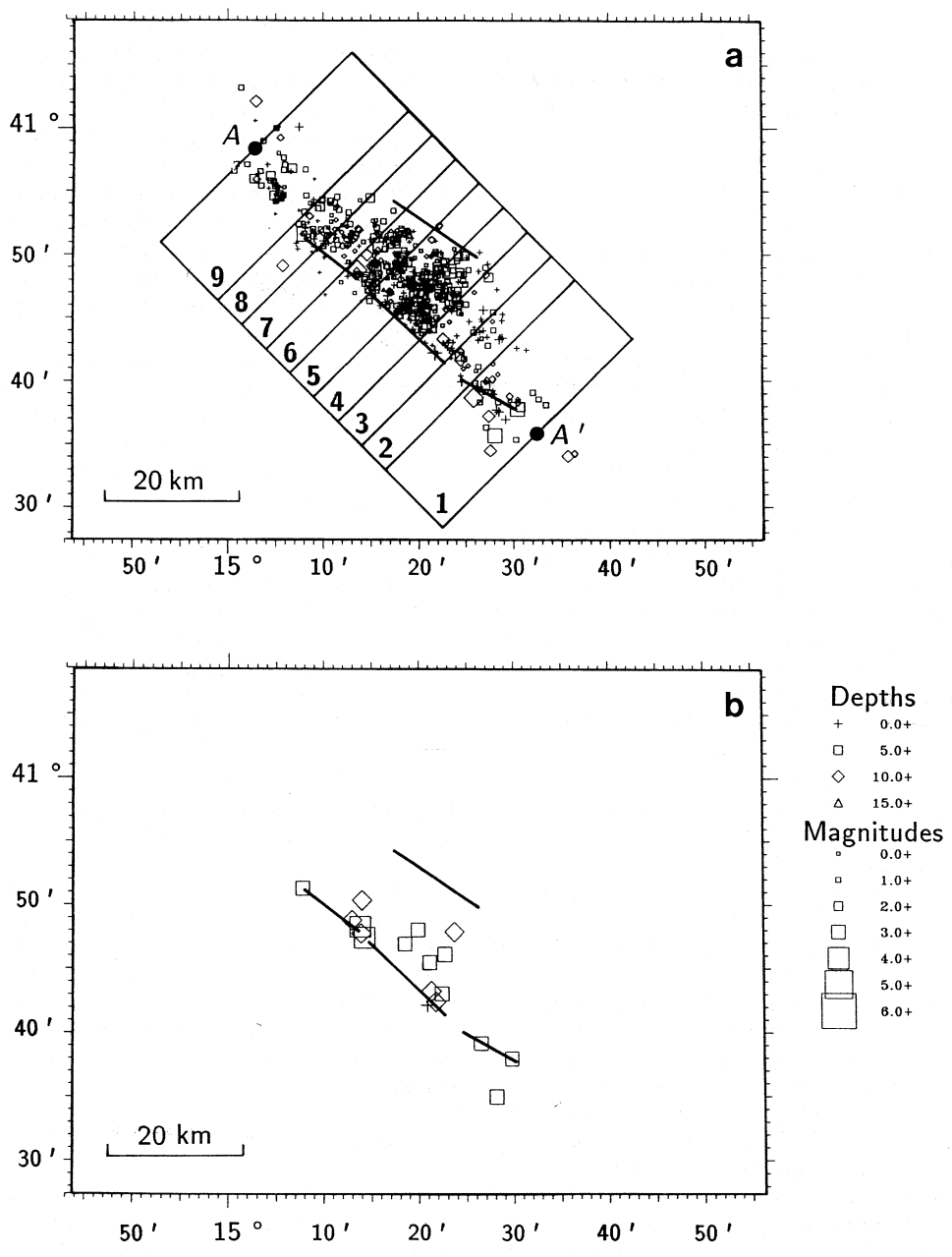

Fig. 6. Aftershocks relocated with the three-dimensional velocity model. In the map a) the lines are the four fault segments proposed by Bernard and Zollo (1989) and Pantosti and Valensise (1990). The boxes 1 through 9 are the vertical sections shown in fig. 7. b) Location of the strongest aftershocks ($M \geq 3.0$). The strongest aftershocks tend to cluster at the edges of the three sub-segments of the main rupture (0 and 20 s episodes).

probably driven by a sharp velocity discontinuity, which is continuous at depth greater than ~6 km, but has lateral variations near the surface. The shallow low-velocity regions (*e.g.*, the Sele Valley) are characterized by no surface rupture and low seismicity, while in the high-velocity regions (*e.g.*, Mt. Marzano) larger surface slip and higher seismicity are observed. The strongest aftershocks seem to cluster at the edges of the sub-segments that ruptured during the mainshock.

The mainshock nucleated in a high-velocity region along a 60° dipping fault that probably steepens from about 7 km depth up to the surface, at the boundary between the stiff Apulian plat-

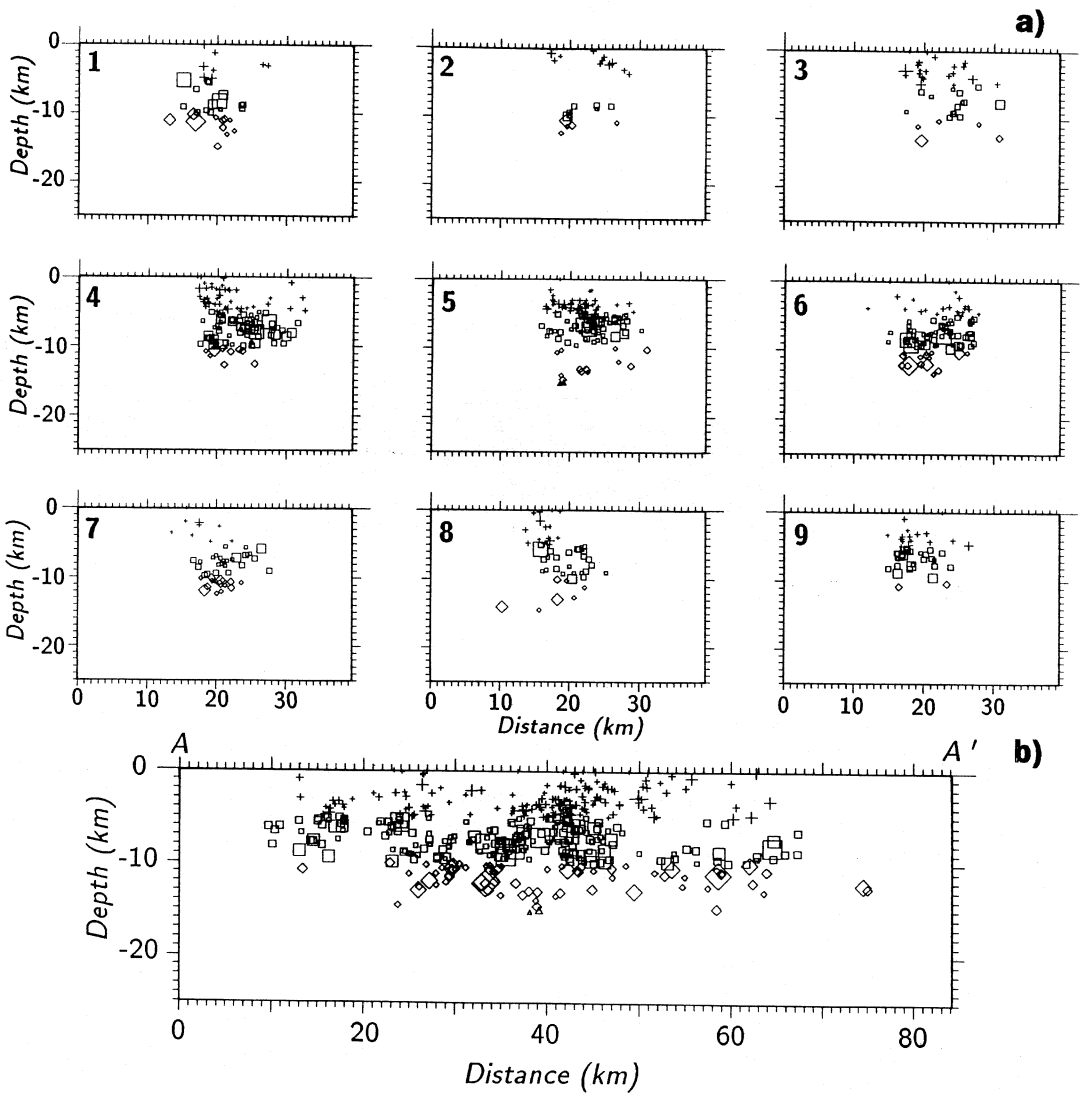

Fig. 7. a) Cross-sections (1 to 9) perpendicular to the main fault of the relocated aftershocks with the three-dimensional velocity model. b) Cross-section parallel to the main fault.

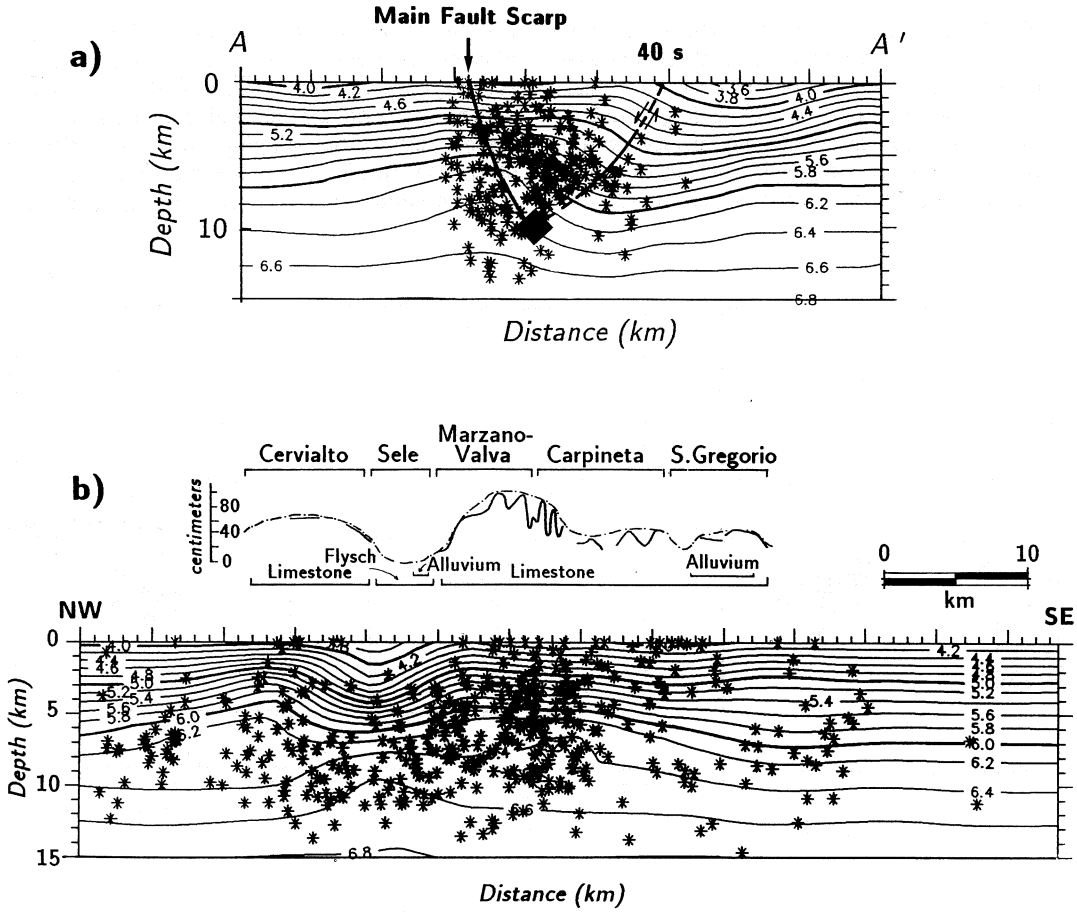

Fig. 8. a) Velocity cross-section perpendicular to the main fault. The rupture started in the high-velocity region, at ~10 km depth (solid diamond), with a 60° dip, and becomes almost vertical in the upper (6÷7) km. «40s» indicates the antithetic fault that ruptured 40 s after the main shock, interpreted as a reactivated thrust. b) Velocity cross-section parallel to the main fault. The seismicity is concentrated beneath the Marzano-Valva sub-segment, where the largest slip (1 m) was observed. The region of the Sele Valley, where no surface slip was observed, is characterized by strong low velocities in coincidence with a lack of seismicity in the upper ~7 km. The surface slip profile is from Pantosti and Valensise (1990).

form and the overlying Meso-Cainozoic sedimentary formations. This northeast-dipping fault is associated with an antithetic fault which ruptured 40 s after the main rupture.

The velocity anomalies suggest that this southwest-dipping normal fault reactivated a thrust of the pre-Pliocene Apenninic compressional tectonics.

REFERENCES

AMATO, A., M. COCCO, D. PANTOSTI and G. VALENSISE (1989): Investigating a complex earthquake with a multidisciplinary approach: the 1980, Irpinia, Normal Faulting event (M_S 6.9), *EOS Transactions A.G.U.*, **70**, 43, 1226 (abstract).

AMATO, A. and G. SELVAGGI (1990): Aftershock relocation and crustal structure in the epicentral region, *Preprints of*

the Proceedings of the International Meeting «Irpinia Dieci Anni Dopo», Sorrento, November 1990, pp. 34-39.

AMBROSETTI, P., C. BOSI, F. CARRARO, N. CIARANFI, M. PANIZZA, G. PAPANI, L. VEZZANI, and A. ZANFERRARI (1983): Neotectonic map of Italy, *Quad. Ric. Sci.*, **114**, 4.

ASTER, R. C. (1986): Hypocenter location and velocity structure in the Phlegrean Fields, Italy, Ph.D. thesis, University of Wisconsin, Madison.

BERNARD, P. and A. ZOLLO (1989): The Irpinia (Italy) 1980 earthquake: detailed analysis of a complex normal fault, *J. Geophys. Res.*, **94**, 1631-1648.

CASERO, P., F. ROURE, L. ENDIGNOUX, I. MORETTI, C. MULLER, L. SAGE, and R. VIALLY (1988): Neogene geodynamic evolution of the Southern Apennines, *Soc. Geol. It., Proceedings of the 74th National Congress, Sorrento.*

COCCO, M. and F. PACOR (1992): The rupture process of the 1980, Irpinia, Italy earthquake from the inversion of strong motion waveforms, *Tectonophysics* (in press).

DESCHAMPS, A. and G.C.P. KING (1984): Aftershocks of the Campania-Lucania (Italy) earthquake of 23 November 1980, *Bull. Seismol. Soc. Am.*, **74**, 2483-2517.

EBERHART-PHILLIPS, D. (1989): Investigations of crustal structure and active tectonic processes in the Coast Ranges, central California, Ph.D. thesis, Stanford University, California.

KLEIN, F.W. (1989): Hypoinverse, a program for Vax computers to solve for earthquake location and magnitude, United States Department of the Interior Geological Survey, open file report 89-314, 6/89 version.

MOSTARDINI, F. and S. MERLINI (1986): Appennino centro meridionale: sezioni geologiche e proposta di modello strutturale, *Soc. Geol. It., Proceedings of the 73rd National Congress, Rome.*

PANTOSTI, D., D.P. SCHWARTZ and G. VALENSISE (1989): Paleoseismologic and geomorphic observations along the 1980 Irpinia surface fault rupture, southern Apennines (Italy), *EOS Transactions A.G.U.*, **70**, 1349.

PANTOSTI, D. and G. VALENSISE (1990): Faulting mechanism and complexity of the 23 November, 1980, Campania-Lucania earthquake inferred form surface observations, *J. Geophys. Res.*, **95**, 15319-15341.

PAVLIS, G.L. and J.R. BOOKER (1980): The mixed discrete-continuous inverse problem: application to the simultaneous determination of earthquake hypocenters and velocity structure, *J. Geophys. Res.*, **88**, 4801-4810.

ROURE, F., P. CASERO and R. VIALLY (1990): Growth processes and melange formation in the southern Apennines accretionary wedge, *Earth Planet. Sci. Lett.* (in press).

THURBER, C.H. (1983): Earthquake locations and three-dimensional crustal structure in the Coyote Lake area, central California, *J. Geophys. Res.*, **88**, 8226-8236.

VALENSISE, G., A. AMATO, L. BERANZOLI, E. BOSCHI, M. COCCO, D. GIARDINI and D. PANTOSTI (1989): Un modello di sintesi del terremoto campano-lucano del 23 novembre 1980, *Proceedings of the G.N.G.T.S. 8th Annual Meeting, Rome.*

VIRIEUX, J., V. FARRA and R. MADARIAGA (1988): Ray tracing for earthquake location in laterally heterogeneous media, *J. Geophys. Res.*, **93**, 6585-6599.

WESTAWAY, R. and J. JACKSON (1987): The earthquake of 1980 November 23 in Campania-Basilicata (Southern Italy), *Geophys. J. R. Astron. Soc.*, **90**, 375-443.